

**Rationalizing accurate structure prediction in the meta-GGA SCAN functional**Julia H. Yang,<sup>1,2</sup> Daniil A. Kitchaev,<sup>3</sup> and Gerbrand Ceder<sup>1,2,\*</sup><sup>1</sup>*Department of Materials Science and Engineering, UC Berkeley, Berkeley, California 94720, USA*<sup>2</sup>*Materials Science Division, LBNL, Berkeley, California 94720, USA*<sup>3</sup>*Materials Department, UC Santa Barbara, Santa Barbara, California 93117, USA*

(Received 20 March 2019; revised manuscript received 5 June 2019; published 26 July 2019)

The ability of first-principles computational methods to reproduce ground-state crystal structure selection is key to their application in the discovery of new materials, and yet presents a formidable challenge due to the low-energy scale of the problem and lack of systematic error cancellation. The recently developed Strongly Constrained and Appropriately Normed (SCAN) functional is notable for accurately calculating physical properties such as formation energies and in particular, correctly predicting ground-state structures. Here, we attempt to rationalize the improved structure prediction accuracy in SCAN by investigating the relationship between preferred coordination environments, the description of attractive van der Waals (vdW) interactions, and the overall ground-state prediction in bulk main-group solids. We observe a systematic undercoordination error in the traditional Perdew, Burke, and Ernzerhof (PBE) functional which is not present in SCAN results and find that semiempirical dispersion corrections in the form of PBE + D3 fail to correct this error in a consistent or physical manner. We conclude that the medium-range vdW interaction is correctly parametrized in SCAN and yields meaningful relative energies between coordination environments.

DOI: [10.1103/PhysRevB.100.035132](https://doi.org/10.1103/PhysRevB.100.035132)**I. INTRODUCTION**

Density-functional theory (DFT) [1,2] provides a robust approximation for the ground-state energy and electron density of a many-body quantum system. It has been broadly useful in a variety of modern materials science challenges such as high-throughput predictions of properties of inorganic systems [3–5], rational design of energy storage materials [6], and in the generation of machine-learning models for studying configurational entropy in multicomponent systems [7]. Answering these types of problems necessarily requires correct prediction of the ground-state crystal structure as it profoundly influences nearly all material properties. However, completely reliable structure prediction remains elusive as the relative energies of competing structures tend to be small and affected by errors arising in various approximations to the exchange-correlation energy.

Approximations to the exchange-correlation energy are often categorized as “rungs of Jacob’s Ladder of density functionals” [8]. The lowest rung refers to the local spin-density approximation (LSDA) and assumes slowly varying electron densities. Despite being constructed to only strictly satisfy the homogeneous electron gas limit, it has found reasonable success in a variety of solids [9–12], although it breaks down in molecular systems [13]. The next ladder rung introduces a dependence on the electron density gradient and is known as the generalized gradient approximation (GGA). One notable GGA is the Perdew, Burke, and Ernzerhof (PBE) functional [14], which has been generally successful in systems where LSDA is lacking [15,16] and is often taken as

a baseline functional for further case-specific corrections. These correction schemes address three major sources of error in PBE: a Hubbard  $U$  term to alleviate self-interaction error, interatomic potentials to introduce van der Waals (vdW) interactions, and fitted elemental corrections to compensate for incomplete error cancellation between condensed phases and their elemental references. A third tier of functionals, referred to as meta-GGAs, introduces a dependence on the Kohn-Sham orbital kinetic energy density. A formal advantage of meta-GGAs is that they are able to recognize all types of orbital overlap, and thereby in principle simultaneously able to represent all types of chemical bonds [17]. The most successful meta-GGA to date is the Strongly Constrained and Appropriately Normed (SCAN) functional [18]. Compared to other nonempirical semilocal-density functionals, SCAN has been shown to yield a significantly more accurate representation of the bulk properties of many semiconducting solids, including but not limited to formation enthalpy [19], bulk modulus, lattice parameter and volume [20], reaction energies [21], and transition pressures [22,23]. However, while SCAN yields accurate properties for strongly bound compounds [24] and ionic systems, it is moderately worse for weakly bound intermetallic compounds [25] and significantly worse than PBE in overestimating magnetic energies in metallic phases [26].

The practical impact of errors in functionals depends very much on what is being compared. An entirely discrete challenge for functionals is the ground-state structure prediction problem because a ground state is either correctly stabilized or not. Only a limited number of case studies are available in the recent literature where SCAN is benchmarked on structure selection, focusing on  $\text{MnO}_2$  [27],  $\text{FeS}_2$  [28],  $\text{Ce}_2\text{O}_3$ ,  $\text{Mn}_2\text{O}_3$ ,  $\text{Fe}_3\text{O}_4$  [29],  $\text{TiO}_2$  [30], as well as broad benchmarking

\*gceder@berkeley.edu

TABLE I. Incorrectly predicted chemistries organized by anion group number. The positive value in parentheses is the absolute value of the energy (in meV/atom) of the DFT-predicted ground-state structure relative to the experimental ground-state structure. Asterisks denote ground states which are polymorphs that have been observed experimentally. A “–” indicates that the ground state is predicted correctly.

Group	PBE (meV/atom)	PBE + D3 (meV/atom)	SCAN (meV/atom)	SCAN + rVV10 (meV/atom)	
15	–	<i>NaP</i> (7.55)	<i>NaP</i> (5.13)	<i>NaP</i> (6.73)	
	–	<i>Na<sub>3</sub>Bi</i> (3.88)	–	–	
16	<i>GeSe</i> (9.25)	<i>GeSe</i> (2.36)	<i>GeSe</i> (1.50)	<i>GeSe</i> (8.79)	
	<i>TeO<sub>2</sub>*</i> (11.08)	<i>TeO<sub>2</sub>*</i> (1.15)	–	–	
	–	<i>GeSe<sub>2</sub></i> (12.50)	–	<i>GeSe<sub>2</sub>*</i> (8.73)	
	<i>SiO<sub>2</sub></i> (10.5)	–	–	–	
	<i>GeO<sub>2</sub>*</i> (2.04)	–	–	–	
	<i>SbO<sub>2</sub>*</i> (1.89)	–	–	–	
	<i>TeO<sub>3</sub></i> (21.61)	–	–	–	
	–	<i>MgTe*</i> (49.98)	–	–	
	17	<i>CaBr<sub>2</sub></i> (20.58)	<i>CaBr<sub>2</sub></i> (13.20)	<i>CaBr<sub>2</sub></i> (6.69)	<i>CaBr<sub>2</sub></i> (5.46)
		<i>SrI<sub>2</sub></i> (27.20)	<i>SrI<sub>2</sub></i> (4.26)	<i>SrI<sub>2</sub>*</i> (7.93)	<i>SrI<sub>2</sub>*</i> (4.38)
<i>SnI<sub>2</sub></i> (33.86)		<i>SnI<sub>2</sub></i> (9.18)	<i>SnI<sub>2</sub></i> (12.98)	<i>SnI<sub>2</sub></i> (5.12)	
<i>BiCl<sub>3</sub></i> (53.35)		<i>BiCl<sub>3</sub></i> (15.30)	<i>BiCl<sub>3</sub></i> (6.41)	–	
–		<i>CaCl<sub>2</sub>*</i> (2.25)	<i>CaCl<sub>2</sub>*</i> (1.63)	<i>CaCl<sub>2</sub>*</i> (3.17)	
<i>SnF<sub>2</sub></i> (2.16)		<i>SnF<sub>2</sub>*</i> (1.79)	–	–	
<i>TlCl*</i> (47.35)		<i>TlCl*</i> (43.08)	<i>TlCl*</i> (3.95)	–	
<i>LiCl</i> (24.95)		<i>LiCl</i> (1.65)	–	–	
<i>CsCl*</i> (47.87)		<i>CsCl*</i> (9.49)	–	–	
<i>TlI*</i> (23.20)		<i>TlI</i> (16.63)	–	–	
–		<i>LiBr*</i> (3.91)	–	<i>LiBr</i> (9.53)	
<i>LiF</i> (4.70)		–	–	–	
<i>BaCl<sub>2</sub>*</i> (24.02)		–	–	–	
<i>SnBr<sub>2</sub></i> (3.05)		–	–	–	
<i>CsBr*</i> (40.13)		–	–	–	
<i>SrBr<sub>2</sub></i> (13.74)		–	–	–	
<i>PbBr<sub>2</sub>*</i> (29.22)		–	–	–	
<i>CsI*</i> (32.20)		–	–	–	
–		–	<i>TlBr</i> (6.81)	–	
–		–	–	<i>SnF<sub>3</sub></i> (13.83)	

work [19] on binary main-group compounds observing that SCAN is more accurate than PBE in ground-state structure prediction. However, there is no established rationalization of the origin of structure prediction accuracy given by the SCAN functional, except in systems where self-interaction is a known problem which can be addressed otherwise through a Hubbard  $U$  correction or higher-order methods.

In this work, we purposely assess the structural errors in main-group closed-shell compounds arising from the PBE functional and explain the origin of accurate ground-state prediction in SCAN. Of the three major sources of error in PBE—self-interaction, lack of vdW, and lack of error cancellation between condensed phases and elemental references—errors in structure selection may only be attributed to the first two factors. We isolate the effect of the vdW term by comparing results from pure PBE and SCAN to that given by a semiempirical D3 vdW correction [31] in order to determine whether either of these conventionally understood sources of error can explain the improvement in structure-selection reliability reported for SCAN. We also include the SCAN + rVV10 functional [32] to determine if long-range corrections can improve structure-selection accuracy in bulk ionic solids. We find that while vdW interactions significantly affect structure selection, a simple vdW correction to PBE yields unphysical

trends in certain chemical spaces. Improvement in structure selection is thus only partially attributable to the presence of a vdW interaction and is highly dependent on the specific parametrization of this interaction. Instead, a consistent indicator of the proper representation of structural energies is the ability of the SCAN functional to choose experimentally consistent coordination environments and unit-cell volumes, leading us to speculate that proper parameterization of the exchange correlation for crystal structure prediction must satisfy both criteria.

## II. METHODS

We base our analysis on 138 binary ionic compounds with formula  $A_xB_y$ , where cation  $A$  is {Li, Na, K, Rb, Cs, Be, Mg, Ca, Sr, Ba, B, Al, Ga, In, Tl, Si, Ge, Sn, Pb} and anion  $B$  is {N, P, As, Sb, Bi, O, S, Se, Te, F, Cl, Br, I}. Together, Table I and Table S1 in Ref. [36] list all the chemistries in this study, and they have also been presented by Zhang *et al.* [19]. Following this reference, we consider experimental structures reported in the Inorganic Crystal Structure Database [33], as well as hypothetical structures derived via ionic substitutions onto likely crystal structures [34]. For example, for materials with chemical formula  $AB$ , the 11 candidate prototypes are listed in Fig. S1 in Ref. [36].

TABLE II. Frequency of structure mis-prediction in PBE, PBE + D3, SCAN, SCAN + rVV10 for 138 main-group compounds.

PBE	PBE + D3	SCAN	SCAN + rVV10
0.15	0.13	0.07	0.07

The prototype of all relaxed structures is investigated using the StructureMatcher functionality in the PYMATGEN code [35] to detect where structures may have relaxed to other prototypes. In particular, we are interested in cases where input structures that were not set up as the experimental structure may have relaxed to the experimental ground state as this can generate false negatives, if not detected. Some of these are shown in Table S2b in Ref. [36]. The case where the experimental input structure relaxes to another type (possible false positive) is also detected. Statistics and examples are shown in Ref. [36]. The site distance threshold in StructureMatcher was set to  $0.3v^{1/3}$ , where  $v$  is the average volume per atom across the two structures. Average coordination numbers are calculated using the crystal nearest-neighbor method in the PYMATGEN code [35], with details and validation given in Ref. [36].

We rely on the Vienna *Ab Initio* Simulation Package (VASP) [37,38] for all calculations, using the same calculation parameters as reported by Zhang *et al.* Specifically, we use projector-augmented wave potentials with a plane-wave cutoff of 520 eV and a reciprocal space discretization of  $25 \text{ \AA}^{-1}$ . We converge all calculations to  $10^{-6}$  eV in total energy and  $0.01 \text{ eV \AA}^{-1}$  in interatomic forces. The pseudopotentials used are listed in Ref. [36] in Table S3. We evaluate all structures with the PBE and SCAN functionals, as well as within the vdW-corrected PBE + D3 and SCAN + rVV10 functionals, and compare the performance of vdW-corrected PBE to the two variants of SCAN. Since the meta-GGA functional uses kinetic-energy densities, a dense  $k$ -mesh may be required. We show in the Supplemental Information convergence with respect to the total number of irreducible  $k$  points [36].

### III. RESULTS AND ANALYSIS

#### A. Dataset overview

We report the ground-state structure mis-prediction rate for the four functionals, where a chemistry is considered incorrectly predicted by a functional if the energy of the experimental ground-state structure is at least 1 meV/atom greater than that of a different structure as determined by the StructureMatcher algorithm. Table II lists these statistics for the 138 main-group compounds.

Table II shows that PBE has the highest mis-prediction rate among the four functionals, and that using the PBE + D3 functional adds a marginal improvement. SCAN reduces the error rate in PBE by half, while SCAN + rVV10 does not offer any improvement over SCAN.

The increased structure-selection accuracy in SCAN can be best appreciated by inspecting the chemistries which are predicted incorrectly by at least one of the four functionals (Table I). Table S1 in Ref. [36] shows the rest of the chemistries that were correctly predicted by all four functionals.

We organize the mis-predicted cases by the anion group number from 15 (pnictide group) to 17 (halide group). Chemistries marked with an asterisk denote structures which have been synthesized experimentally in this chemistry but are not the ground state (e.g., they are known metastable structures), and chemistries with no asterisk are structures which have not been observed experimentally synthesized for that system.

SCAN corrects several of the ground-state errors of PBE, particularly in the halide chemistries which will be discussed in the following sections. Furthermore, in several systems where SCAN predicts an incorrect ground state (e.g., GeSe, CaBr<sub>2</sub>, SrI<sub>2</sub>), it moves the error in the correct direction with respect to PBE. Still, a few errors are increased by SCAN over PBE (NaP, CaCl<sub>2</sub>, TlBr). We discuss a few cases from Table I in more detail below.

#### 1. SrI<sub>2</sub>

Table I shows that the ground-state structure for SrI<sub>2</sub> in all functionals is incorrect. The experimental ground state (space group *Pbca*, sevenfold coordination) has two iodine sites, described as having one I coordinated to Sr in a trigonal plane and the other coordinated to Sr tetrahedrally [39].

The ground state in PBE is a layered structure (space group *P-3m1*) which has not been observed experimentally for this chemistry. Likewise, PBE + D3 predicts a ground state (space group *P-1*) which also has not been seen experimentally. In contrast, the ground state in SCAN and SCAN + rVV10 is the metastable SrI<sub>2</sub> structure (space group *Pnma*) which is synthesized via slow dehydration of its monohydrate form, SrI<sub>2</sub> · H<sub>2</sub>O [40]. This polymorph contains tetrahedral I-Sr and distorted trigonal planar I-Sr environments and the tetrahedral I-Sr symmetry is captured well in SCAN and SCAN + rVV10, unlike in PBE + D3 which distorts the I-Sr tetrahedral bonds, resulting in a lower-symmetry structure. In summary, while no ground states are correctly predicted in any of the functionals, SCAN and SCAN + rVV10 notably predict a successfully synthesized polymorph.

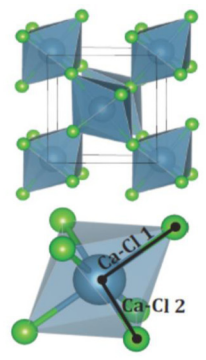
#### 2. CaCl<sub>2</sub>

The ground state of CaCl<sub>2</sub> is orthorhombic (space group *Pnmm*), but it is known that CaCl<sub>2</sub> crystals undergo a second-order ferroelastic transition to the  $\alpha$ -PbO<sub>2</sub> phase at high temperature [41]. The two phases have the same local coordination and only differ in volume by 1%. All functionals except PBE overstabilize this higher-pressure phase by a few meV/atom, and the dispersion-corrected functionals worsen the accuracy by exacerbating the overstabilization of a higher-pressure polymorph.

We also note the geometric features of orthorhombic CaCl<sub>2</sub> as calculated within each functional. Table III describes the two different Ca-Cl distances in the CaCl<sub>6</sub> octahedron and the lattice parameters, showing how the Ca-Cl bond lengths in SCAN are closest to experimental values [42]. Furthermore, in every feature, SCAN never stabilizes a value that is furthest away from the experimental value because it never makes the largest errors, which are colored in red. Meanwhile, PBE makes the largest errors in the Ca-Cl bond lengths, PBE + D3 and SCAN + rVV10 have the largest error in the  $a$ -lattice

TABLE III. Structural features of the orthorhombic  $\text{CaCl}_2$ -structure ground state as determined experimentally [42] and calculated by PBE, PBE + D3, SCAN, and SCAN + rVV10. The two types of Ca–Cl bond lengths are shown in the structure to the right generated by VESTA [44], with the largest bond length deviations from experiment per geometric feature highlighted in red in the table.

	Exp. (Å)	PBE		PBE+D3		SCAN		SCAN+rVV10	
		(Å)	%	(Å)	%	(Å)	%	(Å)	%
Ca-Cl 1	2.74	2.78	1.46	2.73	-0.22	2.74	0	2.73	-0.36
Ca-Cl 2	2.74	2.76	0.73	2.73	-0.21	2.74	0	2.73	-0.36
$a$	4.18	4.19	0.24	4.14	-0.96	4.16	-0.48	4.14	-0.96
$b$	6.44	6.55	1.71	6.48	0.62	6.47	0.47	6.45	0.16
$c$	6.29	6.32	0.48	6.14	-2.38	6.27	-0.32	6.25	-0.64



parameter, PBE has the largest error in the  $b$ -lattice parameter, and PBE + D3 overbinds the most in the  $c$ -lattice parameter. This finding that SCAN improves lattice parameters over PBE is consistent with previous studies [20,43], and we additionally observe that despite the lack of the correct ground state for  $\text{CaCl}_2$ , the structural features of the experimental ground state in SCAN are more accurate than in PBE which is the only functional to stabilize the experimental ground state.

### 3. $\text{SnI}_2$

While the ground state in  $\text{SnI}_2$  is incorrectly predicted across all functionals, the magnitude of error is lowest for PBE + D3 and SCAN + rVV10, followed by SCAN, then PBE. All four functionals stabilize a layered structure (space group  $P-3m1$ ) with octahedral symmetry instead of the monoclinic structure (space group  $C2/m$ ). Howie *et al.* [45] described the structure to contain two distinct metal sites, where two-thirds of the Sn atoms occupy environments similar to that of Pb in the  $\text{PbCl}_2$  structure (i.e., a trigonal prism with an additional bond for a total coordination of seven). The last third of Sn sit in an octahedron where four of the I atoms form  $\text{PdCl}_2$ -type chains and the other two I are slightly further away ( $\sim 0.02$  Å). The  $\text{PdCl}_2$ -type environment is interlocked with the  $\text{PbCl}_2$ -type environment. Howie *et al.* summarized that the structure is layered in a dual sense: first, that the I belonging to both  $\text{PdCl}_2$ -type and  $\text{PbCl}_2$ -type environments form tightly puckered (201) sheets loosely connected by long Sn–I bonds, and second, that crystallographically the structure shows (010) layering. The authors were not able to use Mössbauer spectroscopy on the Sn quadrupoles to resolve the two distinct Sn sites due to a lower-than-expected isomer shift, and concluded that one of the Sn in the unit cell could not be purely ionic. Howie *et al.* suggested that if some  $5s$  electrons are involved in the conduction bands, the Mössbauer spectrum could be better explained. Clearly, the  $\text{SnI}_2$  structure remains to be completely resolved both experimentally and via first-principles methods. While it is possible that a hybrid functional may be able to correctly predict the ground state of  $\text{SnI}_2$ , we find here that SCAN + rVV10 captures the energy of the layered ground-state structure most consistently with ex-

periment. (An extended discussion on ground-state prediction of layered materials will follow.)

### 4. TlBr

The ground state for TlBr is the CsCl structure [46] and correctly predicted by all functionals, except in SCAN, which stabilizes the orthorhombic structure (space group  $Cmcm$ ), a prototype which has not been observed experimentally for this chemistry. In fact, this  $Cmcm$  structure is actually the ground state for TlI, although it can be observed in ternary Tl–Br–I phases,  $\text{TlBr}_{1-x}\text{I}_x$ , where  $x > 0.3$  [47]. The ground state of TlI contains sevenfold-coordinated environments, where five of the bonds are coordinated in a rectangular pyramid (one bond is 3.36 Å and the other four are 3.49 Å) and the last two bonds are longer, at 3.83 Å. Samara *et al.* [48] described this structure to be a compromise between NaCl-type and CsCl-type structures given that both prototypes are ground states for other Tl halides and that the local coordination of  $Cmcm$  takes on an intermediate value of seven. The authors reasoned that the TlI ground state is stabilized through the polarizability of the Tl ion and the tendency for I to make covalent bonds. Based on the structural analysis on TlI by Samara *et al.*, we hypothesize that the SCAN functional may predict more covalent Tl–Br bonds than what is observed experimentally, resulting in an incorrect ground state. Given the small energy differences involved, it is possible that spin-orbit interactions, not included in this work, would modify the structural energetics for these heavy elements.

Only a few cases from Table I have been discussed but they reveal several trends: Sometimes, the predicted ground state has not been observed experimentally in that system, implying that it is not even a metastable phase. This is the case for the  $\text{SrI}_2$  structure predicted by PBE and PBE + D3, the layered  $\text{SnI}_2$  predicted by all four functionals, and the polymorph of TlBr predicted by SCAN; other times, functionals stabilize the higher-pressure polymorph, such as PBE + D3, SCAN, and SCAN + rVV10 for  $\text{CaCl}_2$ . We note that adding dispersion corrections further binds the anions in  $\text{CaCl}_2$  and exacerbates the stabilization of lower-volume polymorphs.

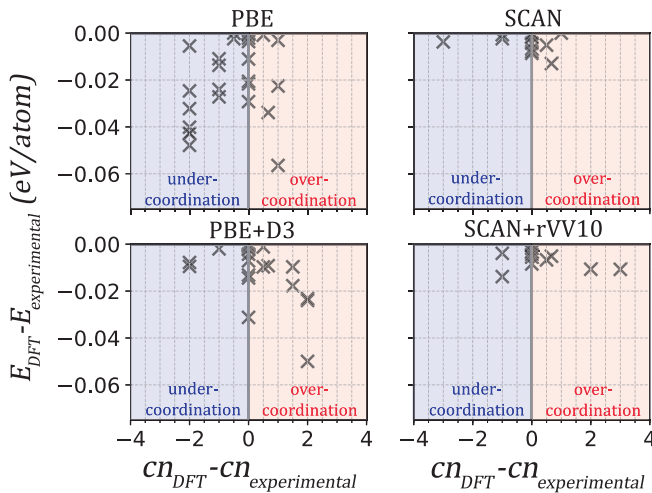


FIG. 1. Cation-anion coordination environments of all incorrectly predicted ground-state chemistries for the four functionals. The x axis is the average  $cn$  of the DFT ground-state structure relative to that of the experimental ground-state structure. The y axis is the DFT overstabilization energy (meV/atom). A negative relative coordination indicates that the functional stabilizes a structure with lower coordination. A positive value means the functional stabilizes a higher coordination.

### 5. General comments

While Table II summarizes that structure selection is on average most accurate in the SCAN functional, Table I alternatively details how certain chemistries are mis-predicted by SCAN but correctly predicted by another functional (in parentheses): NaP (PBE), TlBr (PBE, PBE + D3, SCAN + rVV10), CaCl<sub>2</sub> (PBE). Unfortunately, it does not seem possible *a priori* to state which functional will get the ground state correct, when SCAN does not.

Table I also elucidates why the PBE + D3 functional does not approach the same structure-prediction accuracy despite including dispersion interactions. While some chemistries wrongly predicted in PBE are corrected by both PBE + D3 and SCAN (e.g., LiF, BaCl<sub>2</sub>, SnBr<sub>2</sub>), a number of other chemistries predicted correctly in SCAN are not correctly predicted in PBE + D3 (e.g., TeO<sub>2</sub>, SnF<sub>2</sub>, LiCl). Furthermore, there are even chemistries which are correctly predicted in PBE but not in PBE + D3: Na<sub>3</sub>Bi, GeSe<sub>2</sub>, MgTe, CaCl<sub>2</sub>, LiBr. Surprisingly, the MgTe ground state is incorrectly predicted to be rocksalt in PBE + D3 by around 50 meV/atom below the true ground state. A discussion on this outlier and rationale for why certain chemistries are mis-predicted in PBE + D3 but correctly predicted in PBE is given in Sec. III C.

### B. Structural trends

A trend emerges when all ground states stabilized by each functional are analyzed. Figure 1 shows the average cation-anion coordination in the predicted ground state relative to the average cation-anion coordination in the experimental ground state plotted with the overstabilization energy, which is the energy difference between the DFT ground state and the experimental ground state. By definition this energy is negative. The blue and red regions show when the DFT ground state has

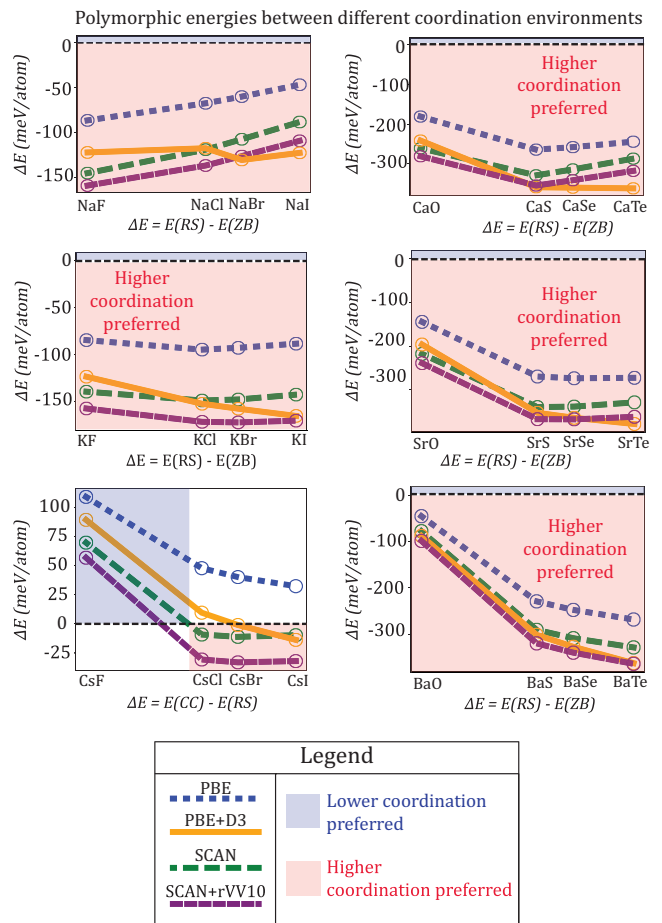


FIG. 2. Energy differences of high- and low-coordination polymorphs for various alkali-halide and alkaline-earth chalcogenides ordered by anion size. The listed structures are rocksalt (RS), wurtzite (WZ), zinc blende (ZB), and cesium chloride (CC). Regions in red indicate the ground state is the higher-coordinated structure while regions in blue indicate the opposite.

a lower or higher coordination than the experimental ground state, respectively. For example, in SrI<sub>2</sub>, where the PBE predicted ground state has a sixfold cation-anion coordination and the experimental structure has a sevenfold cation-anion coordination, the coordination difference predicted by PBE is  $-1$ .

Figure 1 indicates that PBE tends to undercoordinate the cation because many of the PBE ground states have lower relative coordination than the experimental ground state. A number of systems are undercoordinated by at least two bonds in PBE. In fact, this preference for PBE to favor undercoordination is noticeable even when the correct ground state is obtained. Figure 2 shows the relative energies between higher-coordinated (rocksalt) and lower-coordinated (zinc-blende) structures in the Na-halide, K-halide, Ca-chalcogenide, Sr-chalcogenide, and Ba-chalcogenide systems. For all these systems, the experimental ground state is rocksalt. While for the Na, Ca, K, and Sr chemistries in Fig. 2 PBE correctly predicts rocksalt as the ground state, it consistently determines the rocksalt energy advantage to be smaller by tens of meV/atom relative to the other functionals. In the Cs halides,

the PBE error is more dramatic. Here, the energy of the CsCl-type structure (the ground state for CsCl, CsBr, and CsI) is compared to that of the rocksalt structure, which is the ground state for CsF. In this case the preference for undercoordination causes PBE to mis-predict the stable structure for all the bigger halogens.

Figure 2 demonstrates that functionals agreeing on the ground-state structure may still represent relative polymorph stabilities differently. Accurate differences between polymorphs are critical in challenges such as synthesis of metastable compounds [49].

While it would be useful to contextualize these polymorph energies with experimental data, we were not able to find experimental values for polymorph energy differences in alkali halide and alkali-earth chalcogenide structures. Blackman *et al.* [46] give qualitative descriptions of potentially existing polymorphs in CsCl, CsBr, and CsI. Thin films of CsBr and CsI deposited on amorphous substrates at low temperatures showed weak diffraction rings corresponding to the rocksalt structure coexisting with stronger diffraction rings from the cesium-chloride structure. These rocksalt patterns disappeared well before room temperature. However, no calorimetry measurements were performed, so no polymorph energies were given.

With the dispersion correction, PBE + D3 no longer has systematic undercoordination because fewer ground-state structures have negative relative coordination as seen in Fig. 1. In fact, polymorph energies in Fig. 2 show that higher coordination is more preferred in PBE + D3 compared to in PBE since the rocksalt–zinc-blende polymorph energies are shifted down in energy by at least 40 meV/atom. This bias is especially strong in the K halides, Cs halides, Ca chalcogenides, Sr chalcogenides, and Ba chalcogenides.

In contrast, no systematic error in coordination preference is observed in SCAN in either ground-state environments in Fig. 1 or in the polymorph energies in Fig. 2. Since volume and lattice parameters derived in SCAN are found to be closest to experimental values [20,43] and do not have systematic overbinding or underbinding, we suppose that the densities and therefore the coordination environments in SCAN should also be reasonable.

### C. Nonphysical errors in PBE + D3

We examine MgTe, overpredicted in PBE + D3 by 50 meV/atom, and the last set of alkali halides which has yet to be discussed: LiF, LiCl, LiBr, and LiI. While most alkali-containing binary compounds are rocksalt structures, as evidenced in Fig. 2, the ground states for LiBr, LiI, and MgTe are wurtzite.

This preference for lower coordination in LiBr, LiI, and MgTe can be understood by considering the anion-anion distance in structures. The anion-anion distance in a higher-coordinated polymorph is less than the anion-anion distance in a lower-coordinated polymorph, as evidenced by Fig. S4 for all alkali-halide and alkali-earth-chalcogenide compounds. (For example, in LiI the anion-anion distance in rocksalt is 4.247 Å, which is smaller than the anion-anion distance in wurtzite, which is 4.513 Å.) Therefore, with increasing anion radius, structures with larger anion-anion separation

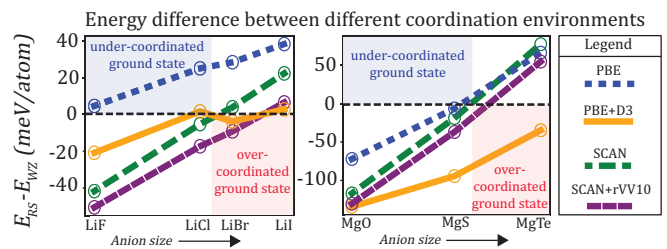


FIG. 3. Energy difference between rocksalt and wurtzite structures for the Li-halide and Mg-chalcogenide chemistries with the four functionals. The colored regions in blue or red emphasize when the ground state is incorrectly predicted to be wurtzite or rocksalt, respectively.

should be energetically favored according to Pauling’s radius ratio rule [50], so we expect a stronger preference for lower coordination.

We assess whether the functionals capture this fundamental trend. Figure 3 shows the polymorphic energy difference between higher- and lower-coordinated structures for the Li-halide and Mg-chalcogenide families as a function of the anion size. The shaded blue or red areas define where a functional stabilizes a structure with lower or higher coordination than the ground state, respectively. For example, since the PBE predicted ground state for LiCl is wurtzite, which is incorrectly positioned 24.95 meV/atom below the true rocksalt ground state, the point for PBE falls in the blue region labeled “undercoordinated ground state.”

From Fig. 3, we observe that as the anion radius increases from F to Cl in the Li halides, the relative stability of the rocksalt structure with respect to wurtzite decreases as expected.

Even PBE which gets the ground states of LiF and LiCl incorrect does capture the trend that with increasing anion size, lower coordination environments should become more stable. Remarkably, the slope of the rocksalt-wurtzite energy difference with anion size is similar for PBE, SCAN, and SCAN + rVV10. Hence, while PBE captures this trend properly, its incorrect prediction of LiCl and LiF seems to stem from an absolute bias towards lower coordination.

In contrast, we observe that PBE + D3 fails to capture the energy dependence on anion size for the Li halides because the slope does not follow the monotonic increase observed in the other three functionals. PBE + D3 in fact demonstrates a systematic preference for higher-coordinated structures since the decreasing stability of the higher-coordinated polymorph with anion size is either absent (K halide, Cs halide, Ca chalcogenide, Sr chalcogenide, Ba chalcogenide) or largely reduced (Li halide, Na halide, Mg chalcogenide) compared to that in other functionals. Hence, while the semiempirical PBE + D3 dispersion appears to reduce the error in PBE by correcting the ground state in LiF and reducing the overstabilization error in LiCl, it confounds polymorphic stabilities and fails to capture fairly basic crystal chemical trends.

### D. Comments on SCAN + rVV10

We find in this study on bulk solids that the long-range vdW contribution in SCAN + rVV10 is dictated, to first order,

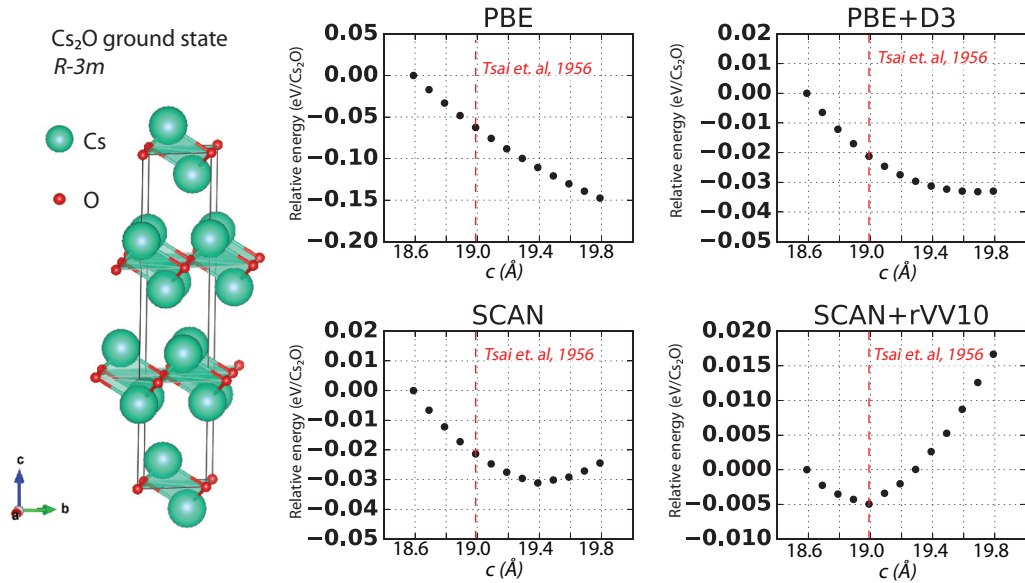


FIG. 4.  $\text{Cs}_2\text{O}$  ground-state structure predicted stability of varying  $c$ -lattice parameter. The experimentally determined value by Tsai *et al.* [51] is indicated by the red dashed line.

by coordination ( $cn$ ) and not by chemistry, meaning that

$$E_{\text{SCAN+rVV10}}(AB, BB, cn) \sim E_{\text{SCAN}}(AB, BB, cn) + vdW^{\text{long-range}}(cn),$$

where  $AB$  indicates cation–anion bonds and  $BB$  indicates non-bonding anion–anion interactions. Since the SCAN + rVV10 polymorph differences in Fig. 2 and Fig. 3 are roughly a constant shift from the SCAN polymorph energies, then it appears that different anion chemistries in the same framework do not contribute additional long-range vdW interactions.

However, this observation may not be true for vdW solids given that dispersion interactions account for a greater fraction of the total cohesive energy in this class of structures. We therefore test SCAN + rVV10 in  $\text{Cs}_2\text{O}$  (space group  $R-3m$ ), a layered material, and compare the results with the other functionals. We calculate the energy of the experimentally determined structure ( $a = b = 4.256 \text{ \AA}$ ,  $c = 18.99 \text{ \AA}$ ,  $\alpha = \beta = 90^\circ$ ,  $\gamma = 120^\circ$ ) [51] and of structures for which the  $c$ -lattice parameter is compressed or expanded. All ions are allowed to fully relax inside a fixed volume cell. Figure 4 shows the predicted  $c$ -lattice parameters, indicating how SCAN + rVV10 most closely agrees with experiment. PBE overestimates  $c$  and predicts the lowest bulk modulus which is a known problem in PBE [52]. PBE + D3 and SCAN overpredict the slab spacing by 0.7 and 0.4  $\text{\AA}$ , respectively.

It is not all that unexpected that the predictions in SCAN + rVV10 for a layered material are closest to experimental values. In a set of 11 representative vdW structures benchmarked with 11 vdW methods, Tawfik *et al.* [53] found that SCAN + rVV10 gives the lowest mean average error for binding energy and  $c$ -lattice spacing and suggested that functionals which include damping functions connecting the dispersion correction to the underlying exchange–correlation functional simply cannot meet the competing demands of both correct energies and correct geometries. In our study, PBE + D3 is such a case in point when compared to SCAN + rVV10.

Additionally, Peng *et al.* [32] benchmarked interlayer spacings and intralayer lattice constants in 28 layered materials which found that SCAN + rVV10 can reproduce interlayer spacing more accurately than SCAN due to the consideration of longer-range vdW in an effective range of 8–16  $\text{\AA}$ . Therefore, the advantage of SCAN + rVV10 over SCAN appears to manifest itself in vdW solids.

#### IV. DISCUSSION

From our detailed study of ground-state prediction in binary ionic compounds where self-interaction is not as prominent as in transition-metal systems, we find that the prediction of ground-state structures in SCAN is on average more accurate than in PBE, PBE + D3, or SCAN + rVV10 (Table I). Furthermore, SCAN does not improperly favor certain metal–anion coordination environments because it neither undercoordinates nor overcoordinates (Fig. 1). In the  $\text{CaCl}_2$  case study in Table III, SCAN most accurately predicts geometric features of the experimental ground state despite understabilizing the structure, even more so than the PBE functional despite it being the only functional to correctly stabilize the ground state.

The reliability of the SCAN functional in predicting ground-state structures is related to its reliability in choosing local environments (i.e., coordination number, connectivity) consistent with experiment. We surmise that a signature of the capability of an exchange–correlation functional to predict crystal structure is a lack of systematic error in coordination number and lattice volume.

It has been argued [18,32] that because the exchange enhancement factor in PBE,  $F_x(s) = 1 + \kappa - \frac{\kappa}{1 + \mu s^2}$ , where  $s = |\nabla n| / (2(3\pi^2)^{1/3} n^{4/3})$ , approaches the Lieb–Oxford bound of 1.804 for large density gradients  $s$ , molecules can lower their energy by moving further apart. We recapitulate this argument in Fig. 5 by plotting the exchange enhancement factor  $F_x$  for

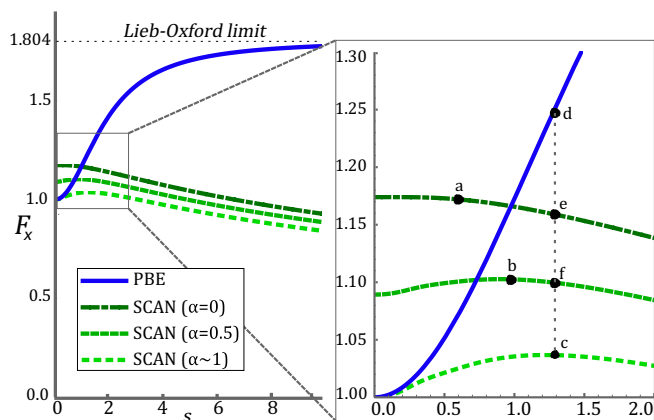


FIG. 5. Exchange enhancement factor,  $F_x$ , for PBE and SCAN for various types of bonding ( $\alpha = 0, 0.5, \sim 1$ ) for large (left) and small (right, figure inset) gradient  $s$ . The points a, b, and c indicate inflection points in  $F_x$  and c, e, and f mark different  $F_x$  for the same gradient  $s$ .

PBE [14] and SCAN [18] for the different types of bonding relevant to this study: covalent ( $\alpha = 0$ ) and ionic ( $0 < \alpha < 1$ ). Since the exchange energy  $E_x[n] = \int d^3r n \epsilon_x^{unif}(n) F_x(s)$  is negative by construction [ $\epsilon_x^{unif}(n) = -(\pi)(3\pi^2 n)^{1/3}$  and  $F_x(s)$  is monotonic and positive], larger density gradients  $s$  always yield a more negative exchange energy. By construction, this form of the exchange artificially lowers the energies in all structures which have maximal electron gradients or minimal electron-electron overlap.

Our study of structure selection focuses on systems with closed-shell anions for which electron density is high on the anion, suggesting that the anion-anion distance, or the extent to which electron densities are nonoverlapping, is the key descriptor for identifying differences among how the functionals evaluate energies. PBE consistently favors minimal electron density overlap, resulting in two possible scenarios: the first is to increase the distance between metal-anion centers, and the second is to include fewer anions in the first anion shell. In fact, both outcomes are observed in our study: (1) the bond lengths in  $\text{CaCl}_2$  as calculated by PBE are always overpredicted (Table III), a known general problem in PBE [52,54]; and (2) there is systematic preference to include fewer anions in the first anion shell, resulting in lower coordination (Fig. 1). We conclude that the analytical form of exchange enhancement factor in PBE artificially shifts structures with those characteristics (large lattice parameters, lower metal-anion coordination) to a lower energy, explaining the high error rate in structure-selection accuracy in the PBE functional.

In contrast, the exchange enhancement factor in SCAN,  $F_x(s, \alpha)$ , does not approach the Lieb-Oxford bound [55,56] for any type of bond or  $\alpha$  value, and also can either favor or disfavor density-density interactions because  $F_x$  contains an inflection point (e.g., points a, b, and c in Fig. 5). The vdW interactions are “activated” at the inflection point, which first prevents the exchange enhancement factor from increasing without bound and second favors density-density interactions, two features crucially missing in PBE. Interestingly,

for decreasing bond strength (increasing  $\alpha$ ), the inflection point occurs at larger density gradient  $s$ , indicating that these intermediate-range vdW interactions in SCAN are sensitive to different types of bonding.

The inset in Fig. 5 also shows how different types of bonding generate greater differences in exchange enhancement factors. For example,  $F_x(s)^{\text{PBE}} - F_x(s, 0.5)^{\text{SCAN}} > F_x(s)^{\text{PBE}} - F_x(s, 0)^{\text{SCAN}}$ , e.g., the difference between points d and f is larger than the difference between d and e. We hypothesize that structure-selection problems involving weakly bound solids where vdW interactions form a greater fraction of the cohesive energy may uncover even greater differences between PBE and SCAN.

We conclude that the origin of the increased accuracy in SCAN in ionic main-group compounds is the inclusion of appropriately parametrized medium-ranged vdW interaction between anions. Since the vdW interaction is attractive, SCAN correctly stabilizes the smaller anion-anion distances in select scenarios, leading to the stabilization of higher-coordinated structures where PBE fails. Thus, the vdW interaction not included in the PBE functional can be reliably accounted for in the SCAN functional.

The semiempirical PBE + D3 correction changes the systematic errors in PBE discussed earlier but does not systematically reduce the structure mis-prediction error because chemistries which are correctly predicted in PBE are sometimes mis-predicted in PBE + D3 (Table I). We reason this anomaly arises from the attractive dispersion on the anions which lowers the energy of structures with shorter anion-anion distances with respect to structures with longer anion-anion distances, a circumstance of the analytical form of the D3 correction. Since anion-anion distances in higher-coordinated structures are consistently shorter than anion-anion distances in lower-coordinated structures (indicated in Fig. S4), PBE + D3 consistently stabilizes higher-coordinated structures.

While for certain cases this correction results in reduced error, such as in LiF and LiCl, in other cases it also leads to mis-prediction, such as LiBr. The consistent stabilization of higher-coordinated structures violates Pauling’s radius ratio rule and fails to reproduce the original polymorph stabilization orderings in PBE (Figs. 2 and 3). Evidently, the D3 correction on average somewhat improves ground-state prediction, but misses classic stability rules.

We speculate that it may be challenging for the semiempirical D3 correction to accurately parametrize the anion-anion interactions based only on the atomic structure and not the electronic (density) structure, which is the method by which SCAN and SCAN + rVV10 include the attractive vdW interactions. In the latter, the long-range vdW correction includes strictly pairwise interactions between volumes of electron densities and maintains a consistent description of polymorphic stabilities across chemical systems because it only contributes a constant energy shift in Figs. 2 and 3.

We conclude that *ab initio* studies of the relative stability of structures necessarily require consideration of vdW forces treated at an electronic density level, as is done in the meta-GGA SCAN functional, as these interactions are critical to structure selection, and empirical forms of vdW attraction based on atomic configuration alone confound physical trends in structure stability.



In this study we purposefully excluded transition metals and rare-earth-containing compounds to separate the self-interaction error from the lack of dispersion in PBE. In fact, several structure-selection studies have pointed out the persistence of the self-interaction error in the SCAN functional because enforcing a Hubbard  $U$  value is necessary to obtain the correct ground state in  $\text{TiO}_2$  [30],  $\text{Ce}_2\text{O}_3$ ,  $\text{Fe}_3\text{O}_4$ , and  $\alpha\text{-Mn}_2\text{O}_3$  [29].

SCAN +  $U$  correctly moves predicted band gaps closer to experimental values by predicting semiconducting behavior instead of metallic behavior in  $\text{Ce}_2\text{O}_3$ ,  $\text{Fe}_3\text{O}_4$ , and  $\alpha\text{-Mn}_2\text{O}_3$ . Interestingly, Gautam and Carter [29] noticed that lower  $U$  values are required in SCAN compared to PBE which they attributed to reduced self-interaction error in SCAN.

Others have uncovered issues in the overestimation of magnetic energies with SCAN. Fu and Singh [26] found that SCAN exaggerates the stability of the Fe body-centered cubic phase by over 0.593 eV/atom and the magnetic moment by 2.63  $\mu_B$ /atom. For elemental V, Co, Ni, and Pd, SCAN also overestimates the magnetic energies and predicts infinite susceptibility for V; therefore, it was concluded that PBE was the more accurate functional for those metallic systems. Additionally, Isaacs *et al.* [25] noticed in intermetallic compounds that SCAN performs moderately worse than PBE with a 20% higher error in formation energy prediction.

A well-regarded functional for the treatment of bulk solids is the PBEsol functional [57], which becomes exact in the limit of solids with slowly varying densities. Hinuma *et al.* [43] compared the performance of seven functionals [PBE, PBE + D3, PBE(+ $U$ ), PBE + D3(+ $U$ ), PBEsol, PBEsol +  $U$ , SCAN] in calculating formation enthalpies, phonon free energies, and lattice parameters of 64 bulk and 25 low-dimensional solids. It was found that PBEsol, SCAN, and PBE + D3 performs the best, even among the low-dimensional materials despite the lack of explicit vdW interactions in PBEsol and SCAN. Mis-prediction of ground states was not discussed in this work.

Therefore, we also compare the accuracy of PBEsol for predicting the ground state in a subset of 45 binary chemistries with that of the other functionals. The comparison of the five functionals for ground-state structure prediction is described in Fig. S2. The results are given as function of an energy window, which is the absolute energy difference between the experimentally determined ground state and the DFT-calculated ground state. This energy window gives an additional metric for analyzing relative energy errors: The greater the energy window necessary to reduce to a zero mis-prediction rate, the greater the magnitude of functional error in ground-state structure prediction. Figure S3 indicates that the PBEsol functional does not approach the same level of structure prediction accuracy as SCAN but is, at least, more accurate than the two other GGA variants (PBE and PBE + D3). Although PBEsol does not explicitly treat vdW interactions, the nonlocality, or  $s$  dependence in the exchange

is actually less pronounced in PBEsol than in PBE, leading to a behavior that is more similar to LDSA. Therefore, lattice constants are not as overestimated in PBEsol [57]. We also plot the exchange enhancement factor of PBEsol in Fig. S3 alongside PBE and SCAN, and notice there are no explicit vdW interactions as there is a lack of an inflection point. Therefore, for binary ionic solids, PBEsol is not expected to reproduce the results given by SCAN.

In our study we include two variants of vdW approximations: semiempirical PBE + D3 and the density-functional approximation SCAN + rVV10. However, there are other vdW methods, such as the fractional ionic approximation (FIA) [58], Tkatchenko-Scheffler (TS) [59], self-consistent screened TS [60], exchange-hole-based correction [61], and others [62] which were not tested.

We do not dismiss the possibility that another GGA-vdW method may yield more accurate statistics than PBE + D3. Certainly, for 11 layered materials, FIA benchmarked against 10 other vdW methods [53] (including SCAN + rVV10 and PBE + D3) gave better energetic and geometric properties than PBE + D3 and at reduced computational cost compared to SCAN + rVV10. It is possible that in some of the layered systems studied in this work, the ground-state prediction accuracy within FIA may be more accurate.

## V. CONCLUSION

Based on a test of 138 main-group compounds where self-interaction error is not prominent, we extract systematic errors in both PBE and PBE + D3 which lead to unphysical trends in structure selection. For PBE, lack of vdW interactions in the exchange energy results in a preference for cation undercoordination. In PBE + D3, the attractive semiempirical vdW correction consistently stabilizes closer-packed anions but does not reproduce known chemical stability rules. We argue that the origin of the increased structure-selection accuracy in SCAN is the chemically sensitive, experimentally consistent representation of medium-ranged vdW attraction. Given the ability of this functional to capture structural stabilities across a wide range of chemistries without demonstrating systematic preference for certain local environments, we recommend SCAN as the functional of choice for evaluating polymorphic stabilities in bulk main-group solids.

## ACKNOWLEDGMENTS

J.H.Y. acknowledges support from the Department of Defense through the National Defense Science & Engineering Graduate Fellowship Program. This work was funded by the US Department of Energy, Office of Science, Office of Basic Energy Sciences, Materials Sciences and Engineering Division under Contract No. DE-AC02-05-CH11231 (Materials Project Program No. KC23MP).

- [1] P. Hohenberg and W. Kohn, *Phys. Rev.* **136**, B864 (1964).  
 [2] W. Kohn and L. J. Sham, *Phys. Rev.* **140**, A1133 (1965).

- [3] A. Jain, S. P. Ong, G. Hautier, W. Chen, W. D. Richards, S. Dacek, S. Cholia, D. Gunter, D. Skinner, G. Ceder, and K. A. Persson, *APL Mater.* **1**, 011002 (2013).

- [4] A. S. Rosen, J. M. Notestein, and R. Q. Snurr, *J. Comput. Chem.* **40**, 1305 (2019).
- [5] S. Sanvito, M. Žic, J. Nelson, T. Archer, C. Oses, and S. Curtarolo, *Handbook of Materials Modeling* (Springer, Cham, 2018).
- [6] D. A. Kitchaev and G. Ceder, *Nat. Commun.* **7**, 13799 (2016).
- [7] A. R. Natarajan and A. Van der Ven, *npj Comput. Mater.* **4**, 56 (2018).
- [8] J. P. Perdew, A. Ruzsinszky, J. Tao, V. N. Staroverov, and G. E. Scuseria, *J. Chem. Phys.* **123**, 062201 (2005).
- [9] M. E. Casida, C. Jamorski, K. C. Casida, and D. R. Salahub, *J. Chem. Phys.* **108**, 4439 (1998).
- [10] C. Stampfl, W. Mannstadt, R. Asahi, and A. J. Freeman, *Phys. Rev. B* **63**, 155106 (2001).
- [11] C. Stampfl and C. G. Van de Walle, *Phys. Rev. B* **59**, 5521 (1999).
- [12] J. K. Labanowski and J. W. Andzelm, *Density Functional Methods in Chemistry* (Springer-Verlag, New York, 1991).
- [13] R. J. Meier, *Comput. Mater. Sci.* **27**, 219 (2003).
- [14] J. P. Perdew, K. Burke, and M. Ernzerhof, *Phys. Rev. Lett.* **77**, 3865 (1996).
- [15] A. D. Becke, *Phys. Rev. A* **33**, 2786 (1986).
- [16] A. D. Becke, *The Challenge of d- and f-Electrons: Theory and Computation*, edited by D. R. Salahub and M. C. Zerner (American Chemical Society, Washington, DC, 1989), Chap. 12, pp. 165–179.
- [17] J. Sun, B. Xiao, Y. Fang, R. Haunschild, P. Hao, A. Ruzsinszky, G. I. Csonka, G. E. Scuseria, and J. P. Perdew, *Phys. Rev. Lett.* **111**, 106401 (2013).
- [18] J. Sun, A. Ruzsinszky, and J. P. Perdew, *Phys. Rev. Lett.* **115**, 036402 (2015).
- [19] Y. Zhang, D. A. Kitchaev, J. Yang, T. Chen, S. T. Dacek, R. A. Sarmiento-Pérez, M. A. L. Marques, H. Peng, G. Ceder, J. P. Perdew, and J. Sun, *npj Comput. Mater.* **4**, 9 (2018).
- [20] G. X. Zhang, A. M. Reilly, A. Tkatchenko, and M. Scheffler, *New J. Phys.* **20**, 063020 (2018).
- [21] C. J. Bartel, A. W. Weimer, S. Lany, C. B. Musgrave, and A. M. Holder, *npj Comput. Mater.* **5**, 4 (2019).
- [22] C. Shahi, J. Sun, and J. P. Perdew, *Phys. Rev. B* **97**, 094111 (2018).
- [23] N. Sengupta, J. E. Bates, and A. Ruzsinszky, *Phys. Rev. B* **97**, 235136 (2018).
- [24] A. Chakraborty, M. Dixit, D. Aurbach, and D. T. Major, *npj Comput. Mater.* **4**, 60 (2018).
- [25] E. B. Isaacs and C. Wolverton, *Phys. Rev. Mater.* **2**, 063801 (2018).
- [26] Y. Fu and D. J. Singh, *Phys. Rev. Lett.* **121**, 207201 (2018).
- [27] D. A. Kitchaev, H. Peng, Y. Liu, J. Sun, J. P. Perdew, and G. Ceder, *Phys. Rev. B* **93**, 045132 (2016).
- [28] M. Y. Zhang, Z. H. Cui, and H. Jiang, *J. Mater. Chem. A* **6**, 6606 (2018).
- [29] G. S. Gautam and E. A. Carter, *Phys. Rev. Mater.* **2**, 095401 (2018).
- [30] Y. Zhang, J. W. Furness, B. Xiao, and J. Sun, *J. Chem. Phys.* **150**, 014105 (2019).
- [31] S. Grimme, J. Antony, S. Ehrlich, and H. Krieg, *J. Chem. Phys.* **132**, 154104 (2010).
- [32] H. Peng, Z.-H. Yang, J. P. Perdew, and J. Sun, *Phys. Rev. X* **6**, 041005 (2016).
- [33] A. Belsky, M. Hellenbrandt, V. L. Karen, and P. Luksch, *Acta Crystallogr., Sec. B: Struct. Sci.* **58**, 364 (2002).
- [34] G. Hautier, C. Fischer, V. Ehrlicher, A. Jain, and G. Ceder, *Inorg. Chem.* **50**, 656 (2011).
- [35] S. P. Ong, W. D. Richards, A. Jain, G. Hautier, M. Kocher, S. Cholia, D. Gunter, V. L. Chevrier, K. A. Persson, and G. Ceder, *Comput. Mater. Sci.* **68**, 314 (2013).
- [36] See Supplemental Material at <http://link.aps.org/supplemental/10.1103/PhysRevB.100.035132> for convergence behavior, comparison with the PBEsol functional, and other calculation details.
- [37] G. Kresse and J. Furthmüller, *Phys. Rev. B* **54**, 11169 (1996).
- [38] G. Kresse and J. Furthmüller, *Comput. Mater. Sci.* **6**, 15 (1996).
- [39] S. A. Hodorowicz and H. A. Eick, *J. Solid State Chem.* **46**, 313 (1983).
- [40] G. Liu and H. A. Eick, *Journal Less-Common Met.* **156**, 237 (1989).
- [41] H. G. Unruh, D. Mühlenberg, and Ch. Hahn, *Z. Phys. B: Condens. Matter*, **86**, 133 (1992).
- [42] C. J. Howard, B. J. Kennedy, and C. Curfs, *Phys. Rev. B* **72**, 214114 (2005).
- [43] Y. Hinuma, H. Hayashi, Y. Kumagai, I. Tanaka, and F. Oba, *Phys. Rev. B* **96**, 094102 (2017).
- [44] K. Momma and F. Izumi, *J. Appl. Crystallogr.* **44**, 1272 (2011).
- [45] R. A. Howie, W. Moser, and I. C. Trevena, *Acta Crystallogr.* **28**, 2965 (1972).
- [46] M. Blackman and I. H. Khan, *Proc. Phys. Soc.* **77**, 471 (1961).
- [47] A. V. Churilov, G. Ciampi, H. Kim, W. M. Higgins, L. J. Cirignano, F. Olschner, V. Biteman, M. Mincello, and K. S. Shah, *J. Cryst. Growth* **312**, 1221 (2010).
- [48] G. A. Samara, L. C. Walters, and D. A. Northrop, *J. Phys. Chem. Solids* **28**, 1875 (1967).
- [49] W. Sun, S. T. Dacek, S. P. Ong, G. Hautier, A. Jain, W. D. Richards, A. C. Gamst, K. A. Persson, and G. Ceder, *Sci. Adv.* **2**, e1600225 (2016).
- [50] L. Pauling, *J. Am. Chem. Soc.* **69**, 542 (1947).
- [51] K. R. Tsai, P. M. Harris, and E. N. Lassetre, *J. Phys. Chem.* **60**, 338 (1956).
- [52] P. Haas, F. Tran, and P. Blaha, *Phys. Rev. B* **79**, 085104 (2009).
- [53] S. A. Tawfik, T. Gould, C. Stampfl, and M. J. Ford, *Phys. Rev. Mater.* **2**, 034005 (2018).
- [54] Y. Zhao and D. G. Truhlar, *J. Chem. Phys.* **128**, 184109 (2008).
- [55] J. P. Perdew, A. Ruzsinszky, J. Sun, and K. Burke, *J. Chem. Phys.* **140**, 18A533 (2014).
- [56] E. H. Lieb and S. Oxford, *Int. J. Quantum Chem.* **19**, 427 (1981).
- [57] J. P. Perdew, A. Ruzsinszky, G. I. Csonka, O. A. Vydrov, G. E. Scuseria, L. A. Constantin, X. Zhou, and K. Burke, *Phys. Rev. Lett.* **102**, 039902(E) (2009).
- [58] T. Gould, S. Lebègue, J. G. Ángyán, and T. Bucko, *J. Chem. Theor. Comput.* **12**, 5920 (2016).
- [59] A. Tkatchenko and M. Scheffler, *Phys. Rev. Lett.* **102**, 073005 (2009).
- [60] A. Tkatchenko, R. A. DiStasio, R. Car, and M. Scheffler, *Phys. Rev. Lett.* **108**, 236402 (2012).
- [61] S. N. Steinmann and C. Corminboeuf, *J. Chem. Phys.* **134**, 044117 (2011).
- [62] J. Harl, L. Schimka, and G. Kresse, *Phys. Rev. B* **81**, 115126 (2010).